ELSEVIER

Biophysical Chemistry 55 (1995) 239–245

Biophysical Chemistry

Solution X-ray scattering study of reconstitution process of tobacco mosaic virus particle using low-temperature quenching ☆

Yoh Sano [a,*], Hideo Inoue [b], Yuzuru Hiragi [c], Hiroshi Urakawa [d], Kanji Kajiwara [d]

[a] *National Food Research Institute, Ibaraki, Japan*
[b] *Shimadzu Corporation, Kyoto, Japan*
[c] *Institute for Chemical Research, Kyoto University, Uji, Japan*
[d] *Kyoto Institute of Technology, Kyoto, Japan*

Received 26 September 1994; revised 16 December 1994; accepted 20 December 1994

Abstract

The reconstitution process of tobacco mosaic virus (TMV) was investigated by the solution X-ray scattering measurements with the synchrotron radiation source using low-temperature quenching. TMV assembly in an aqueous solution is completely stopped below 5° C. The TMV assembly was traced by the small-angle X-ray scattering (SAXS) measurements at 5° C on a series of solutions prepared by low-temperature quenching after incubation either at 15, 20 or 25° C for an appropriate interval between 0 and 60 min. The SAXS results were analyzed by the Guinier plot, the Kratky plot and the distance distribution function. In order to account the time course of SAXS profiles in terms of the elongation of TMV assembly, a model calculation was performed to simulate the Guinier plot, the Kratky plot and the distance distribution function by applying Glatter's multibody method using models that were constituted of the spheres representing a column of piled two-layer disks of TMV-protein. The three simulated functions thus obtained support the conclusion derived from the three functions calculated from the experimental results that the incubation of the RNA and protein of TMV began to reconstitute TMV instantly after mixing, proceeded steeply to a long rod, and then extended asymptotic to the full length of the TMV particle. This process is in good agreement with that obtained from electron microscopic studies.

Keywords: Solution X-ray scattering; Tobacco mosaic virus; Reconstitution; Quenching

1. Introduction

Tobacco mosaic virus (TMV) is one of the well-characterized plant viruses, and consists of single-stranded RNA of ca. 6400 nucleotides long surrounded by a single type of coat protein of ca. 2100 subunits [1,2]. It forms a hollow cylinder of a length of 3000 Å, inner diameter of 40 Å, and an outer diameter of 180 Å. The TMV particle can be reconstituted in vitro from its constituents under physiological conditions in two steps of nucleation and elongation [3–5]. TMV-RNA has a specific region at about 900 nucleotides from the 3′-end that is capable of forming a weakly base-paired stem with a loop [6]. First, nucleation is considered to take place by

☆ This work has been performed under the approval of the Photon Factory Program Advisory Committee (proposal nos. 90-192 and 90-194). This work was supported in part by a grant from the Science and Technology Agency of Japan.

* Corresponding author.

SSDI 0301-4622(95)00003-8

the insertion of this hairpin loop into the central hole of the nucleating two-layer disk of which two rings are opened apart onto the hole. We use the term 20S disk to refer to the two-layer, 17 subunits per layer, cylindrical structure sedimenting at about 20S. Elongation then follows in the two directions. The longer 5′-tail is fold back down the central hole of the rod and forms a special structure, a travelling loop, which is essential for the most rapid elongation in this direction. As long as this structure is maintained, elongation towards the 5′-end appears to proceed from subunits in disks or some smaller aggregates. After the 5′-tail is encapsidated with the coat protein, a protein composed of small aggregates, collectively known as A-protein, appears to add along the 3′-tail of the RNA, which protrudes directly from one end of the growing rod. The formation of nucleation between the hairpin loop of the RNA and the double-layered disk is instantaneous, whereas the elongation process is in the range of minutes and has two steps. While elongation toward the 5′-tail takes about 5–7 min, that toward the 3′-tail is completed in 20–40 min. The time course of TMV assembly was measured mainly by electron microscopy, turbidimetry, pulse–chase measurements etc. [7–12]. It is not possible to perform a real-time observation of the elongation process of the assembly, in particular, the helix formation of RNA with coat proteins by these methods. This may be attainable by using both two methods of time-resolved small-angle neutron (SANS) and X-ray scattering (SAXS) measurements. Both methods can offer information about the tertiary structures of the virus *in solutions*, i.e., in physiological conditions. Neutron scattering is now firmly established as an invaluable complement to X-ray scattering for structural and dynamic studies in the fields of biology and polymer science. Small-angle neutron scattering measurement enables us to determine the internal conformational relationship between RNA and protein in virus particles using the contrast variation method [13]. Therefore, if we apply both methods to follow the TMV assembly reaction, we can elucidate the self-assembling kinetics, i.e., the elongation speed of TMV particles and its components, RNA and protein, separately.

At present the time-resolved SAXS method is available at, for example, the Photon Factory in the National Laboratory for High Energy Physics (KEK), Japan [14], but the time-resolved SANS method cannot be applied for the TMV assembly because of the relatively fast assembly reaction and insufficient neutron intensity to follow it. However, the TMV assembly in an aqueous solution can be stopped below 5° C [15,16]. If a reaction mixture of TMV-RNA and TMV-protein kept at 25° C is quenched into ice water, for instance, at 10 min after mixing, this quenched mixture maintains the assembly state at 10 min as long as it is kept at 5° C. Therefore, we can trace the TMV reconstitution process by carrying out SAXS or SANS measurements on a series of reaction solutions quenched at 5° C with appropriate time intervals. We refer this method as a low-temperature quenching. The present paper will describe measurements of SAXS with the synchrotron radiation X-ray source on TMV assembly process using low-temperature quenching.

2. Materials and methods

2.1. Preparation of TMV and its components, RNA and protein

Tobacco mosaic virus, Japanese common strain OM [17] was propagated in inoculated leaves of *Nicotiana tabacum* L. cv. Xanthi. Leaves harvested 7–10 days after inoculation were homogenized with 100 mM phosphate buffer (pH 7.0) containing 0.1% (v/v) thioglycolic acid. The virus was collected by polyethylene glycol precipitation [18] and purified by two cycles of differential centrifugation. RNA was isolated from the purified virus by phenol/bentonite extraction [19]; coat protein was isolated by the acetic acid method [20]. Coat proteins were dialysed against the experimental buffer (100 mM sodium phosphate, pH 7.2) at 4° C and used immediately. The concentration of the protein used was adjusted to 20.0 $mg \cdot ml^{-1}$, and that of RNA was to 1.0 $mg \cdot ml^{-1}$, because the weight ratio of RNA to protein in TMV is 1:20. The concentrations of TMV, RNA and protein were determined spectrophotometrically by using an absorptivity value of 3.0 $ml \cdot cm^{-1} \cdot mg^{-1}$ at 260 nm for the virus, 20.0 $ml \cdot cm^{-1} \cdot mg^{-1}$ at 258 nm for the RNA [21], and 1.27 $ml \cdot cm^{-1} \cdot mg^{-1}$ at 282 nm for the protein [22].

2.2. Low-temperature quenching method

After mixing each 5 ml of RNA and protein solution in a tube at 5°C, the tube was immersed into a thermostat at either temperature of 15, 20, or 25° C. At an appropriate time interval between 0 and 60 min, each 0.5 ml of the reaction solution was subtracted from the tube and was quenched in ice water below 5° C as quick as possible. The elongation reaction was completely stopped by quenching at 5° C [15,16]. We have performed SAXS measurements at 5° C on each of the quenched solutions to determine the degree of elongation.

2.3. Small-angle X-ray scattering measurements

SAXS experiments were carried out at 5° C with the optics and detector system of SAXES (small-angle X-ray scattering equipment for solution) [23] installed on the 2.5 GeV storage ring in the Photon Factory, KEK, Tsukuba, Japan. Scattering intensities were registered at 512 different angles with a wavelength, λ, of 1.49 Å in the range $0.013\ \text{Å}^{-1} < Q < 0.335\ \text{Å}^{-1}$, where Q denotes the amplitude of the scattering vector equal to $4\pi \sin\theta/\lambda$ and 2θ is the scattering angle. The SAXS experimental procedure was described in details elsewhere [24]. The important condition was to keep the specimen chamber at 5° C throughout the experiments in order to prevent the elongation reaction. The SAXS intensity was measured for 300 s for all the solutions and buffers, and the net scattering intensities were calculated by subtracting the scattering intensities of a blank buffer solution from those of the assembly solutions.

3. Results

3.1. Guinier plots

The radius of gyrations, R_g, is a useful parameter to observe the growth of a rod-shaped particle. When the logarithms of the X-ray scattering intensity at Q, $J(Q)$ are plotted against the square of Q (the Guinier plot [25]), a linear line is usually drawn in the range of $Q \cdot R_g \leqslant 1$, and its slope gives a value of R_g. The TMV assembly solutions observed contain different degrees of elongation, and thus the R_g evaluated

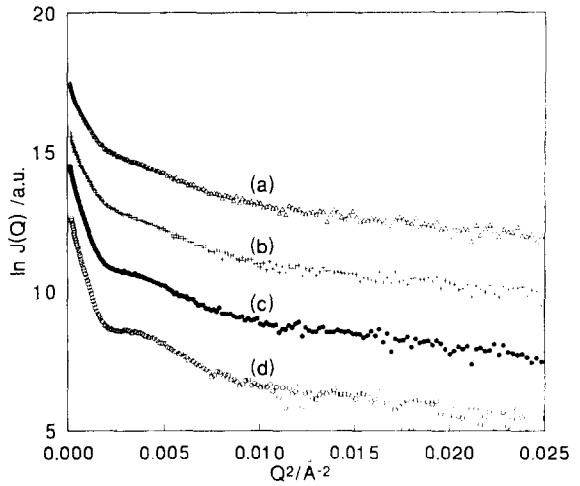

Fig. 1. Guinier plots derived from the TMV assembly process at 20° C. The TMVP solution was quenched at (a) 0 min (tr 00), (b) 2 min (tr 02), (c) 8 min (tr 08), and (d) 25 min (tr 25) after mixing RNA at 20° C.

from SAXS measurements corresponds to the z-average radius of gyration, $R_{g,z}$ [24]. Fig. 1 shows the Guinier plots of a series of TMV assembly samples as an example, quenched at 0, 2, 8 and 25 min after mixing at 20° C. In a low Q range a straight line was depicted in each Guinier plot, and its slope yields $R_{g,z}$. An initial slope increases with incubation time at 20° C, and a peak at around $Q^2 = 0.003\ \text{Å}^{-2}$ becomes steeper. The time courses of the radius of gyration is shown in Fig. 2 for TMV assembly solutions being incubated at 15, 20 and 25° C. R_g(TMVP) and R_g(TMVP + RNA) denote the radius of gyration in the solutions containing only the coat protein and the protein plus RNA, respectively. The value of the radius of gyration R_g(TMVP + RNA) increases more rapidly at 20° C with the incubation time, compared to that at either 15° C or 25° C, while the value of R_g(TMVP) hardly changes with time.

3.2. Kratky plot

In synthetic polymer chemistry the Kratky plot is usually employed to evaluate the shape and the order of extension of a linear or branched-chain polymer [26]. Even if polymers have the same R_g value in solution, Kratky plots reveal the difference according

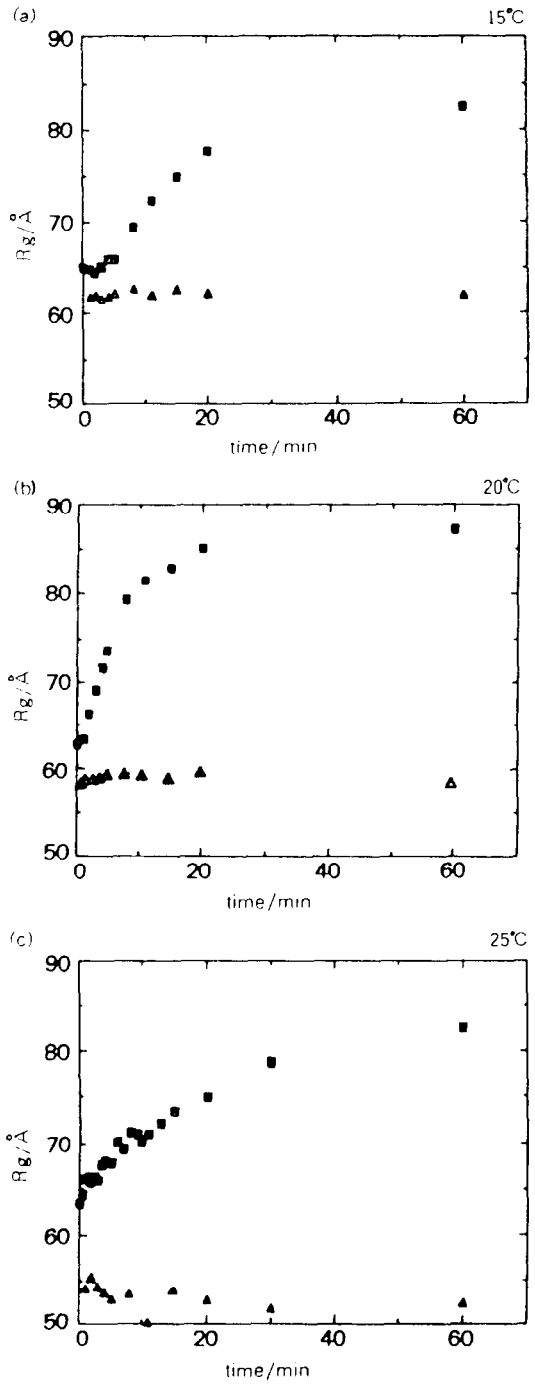

Fig. 2. Time course of the radius of gyration, R_g, during TMV assembly at (a) 15° C, (b) 20° C, and (c) 25° C. (▲) R_g (TMVP) and (■) R_g (TMVP + RNA) denote the radius of gyration in the solutions containing only the protein and the protein plus RNA of TMV, respectively.

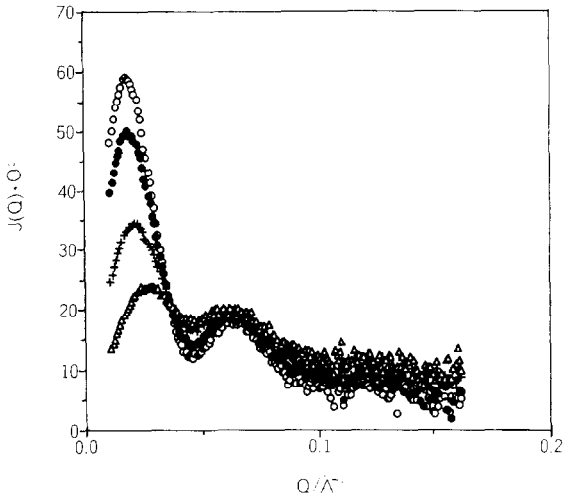

Fig. 3. Time variation of the Kratky plots during TMV assembly at 20° C. (△) 1 min, (+) 5 min, (●) 11 min, and (○) 25 min incubation times, respectively.

to their shape and chain extension (e.g., a spherical shape yields a sharp peak, a Gaussian chain a horizontal line and a rigid rod a straight line with a slope one). The Kratky plot is obtained by plotting the X-ray scattering intensity $J(Q)$ times the square of Q against Q, and is more sensitive than the Guinier plot to the changes in polymer chain configuration. Fig. 3 depicts the time variation of Kratky plots during TMV assembly at 20° C, where the SAXS data are obtained from the solutions quenched at 1 min (tr 01), 5 min (tr 05), 11 min (tr 11) and 25 min (tr 25). A pronounced increase is observed in the first peak at around 0.02 $Å^{-1}$, whereas the second peak is almost invariant at about 0.07 $Å^{-1}$. A similar time variation in the Kratky plots was obtained for the TMV assembly at 15° C and at 25° C (data not shown).

3.3. Distance distribution function

Another index of polymer chain conformation is a distance distribution function, $p(r)$, defined by Eq. (1).

$$p(r) = (1/2\pi^2)\int_0^\infty J(Q)(Qr)\sin(Qr)\mathrm{d}Q \qquad (1)$$

This function is obtained by Fourier-transforming the X-ray scattering intensity function, $J(Q)$, multiplied

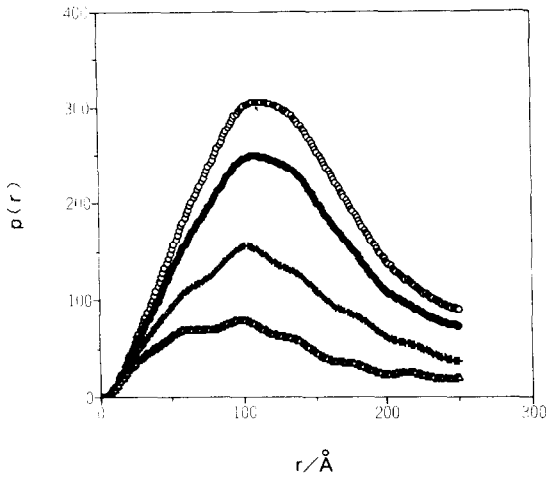

Fig. 4. Time variation of the distance distribution function during TMV assembly at 20° C. (△) 1 min, (+) 5 min, (●) 11 min, and (○) 25 min incubation times, respectively.

with $Q \cdot r$ [27], and represents a statistical distribution function of a pair of points being separated by a distance of r Å within a polymer molecule.

The distance distribution function changes with the incubation time as shown in Fig. 4 during TMV assembly at 20° C for 1, 5, 11 and 25 min after mixing of TMV-RNA with the protein, where the symbols in Fig. 4 are the same as in Fig. 3. A relative ratio of $p(r)$ at around 100 Å to that at around 60 Å was found to increase gradually with the incubation time. A similar incubation-time dependence in the distance distribution function was observed during the TMV assembly at 15° C and 25° C (data not shown), as expected from the Kratky plots.

4. Discussion

The results calculated from the SAXS measurements on TMV assembling solutions, (i.e., the time variations in the radius of gyration, the Kratky plot and the distance distribution function) indicate that at the incubation of TMV-RNA and TMV-protein at 20° C the reconstitution of TMV starts immediately after mixing, and proceeds fast enough to form a long rod during the first 10 to 20 min. The full length of TMV particle seems to be formed in 40 to 60 min in this condition.

The effect of the incubation temperature on TMV assembly is qualitatively seen in Fig. 2. When no RNA was added, the radius of gyration of the protein R_g (TMVP) exhibited almost no change during incubation at 15, 20 and 25° C. As already published in Fig. 3 of [14], the radius of gyration R_g increased up to 65 Å at 5 mg/ml protein concentration in 100 mM phosphate buffer at the same condition in this paper within 1 s after bringing the protein solutions from 5° C to 20° C or 25° C, and its value gradually increased and almost saturated at about 30 s. The radius of gyration of 20S disk is calculated as 66.5 Å with a suitable model as mentioned in [24], so that 20S disk would have actually been formed at very early stage within a few seconds even at a 5 mg/ml concentration during the sample preparation prior to SAXS measurements. When RNA was added, the R_g (TMVP + RNA) value was found to increase rapidly in the first 20 min and then gradually approached a finite value. A rise in the incubation temperature from 15° C to 20° C resulted in a steeper increase in R_g at the first stage, and in a larger R_g value (87.1 Å) at an incubation time of 60 min, as compared with the maximum value of R_g 82.6 Å at 15° C. A further rise in the temperature to 25° C induced a rather slow increase in the R_g value at the initial stage, and led to a lower value (82.6 Å) at 60 min. As described in the Introduction, the TMV assembly is thought to be induced by a formation of the initial complex, which is composed of RNA entrapped in the hollow of a 20S disk. Since TMV-protein tends to aggregate to longer 2- and 3-layered 20S disks rather than single-layered 20S disk [24] at 25° C, the slower increase in R_g at 25° C is attributed to less 20S disks available for the nucleation (initial RNA-protein complex formation) to initiate the TMV assembly.

Although a radius of gyration evaluated from the Guinier plot is a sensitive parameter to indicate a change in a molecular volume, this parameter is not suitable as a measure of elongation of a long rod. We have employed, therefore, the Kratky plot and the distance distribution function for this purpose. Both functions exhibited a growth in rod length of the assembly with the incubation time, as seen in Figs. 3 and 4. It is observed that a ratio of the first peak to the second peak changes with the incubation time in the Kratky plot and $p(r)$ function, and that the side peak of the Guinier plot at about 0.003 Å^{-2} in Fig. 1

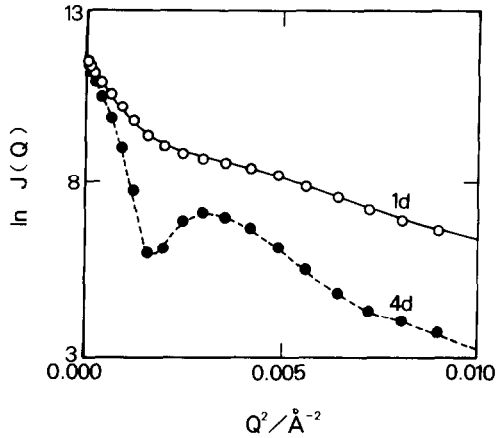

Fig. 5. Simulated Guinier plot for the model representing the multi-layered 20S disk of TMV protein. Symbols 1d and 4d denote a 20S disk and 4-layered 20S disk, respectively.

becomes steeper with the time. In order to correlate the time course of the three functions at least qualitatively with the elongation of TMV assembly, we have simulated the time variation in the three functions using the Glatter's multibody method [28]. First, we construct a three-dimensional lattice space with 4 Å spacing, and place a sphere of radius 2.48 Å at each lattice point according to a model to be calculated. Second, we calculate the scattering X-ray intensity, $J(Q)$, from the model composed of spheres. Third, the Guinier plot, Kratky plot and distance distribution function all can be computed from $J(Q)$. Four types of models were used in this case: single-layered 20S disks, 2-layered 20S disks, 3-layered 20S disks, and 4-layered 20S disks of TMV-protein of which the dimension was described elsewhere [24]. The simulation by the Glatter's multibody method yielded the Guinier plot, the Kratky plot and the distance distribution function, respectively, as shown in Figs. 5–7 for 1- to 4-layered 20S disks. The simulated curves of the Guinier plot in Fig. 5 indicate that a peak appears in the model of the 4-layered 20S disk, and the peak intensity increases with the further growth of disks. Accordingly the increase in the side peak intensity at about 0.003 $Å^{-2}$ in Fig. 1 confirms the elongation of the TMV assembly.

The simulated Kratky plots for the multi-layered 20S disks (Fig. 6) exhibit two peaks in the small angle range at about 0.02 $Å^{-1}$ and 0.07 $Å^{-1}$, which were also observed experimentally (see Fig. 3). As

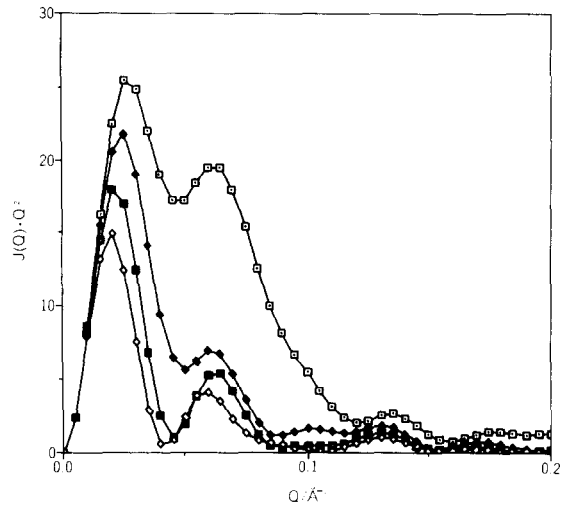

Fig. 6. Simulated Kratky plots for the model representing the multi-layered 20S disks of TMV protein. (⊡) 1d, (♦) 2d, (■) 3d and (◇) 4d denote a 20S disk, 2-layered 20S disk, 3-layered 20S disk and 4-layered 20S disk, respectively.

the calculated values of $J(Q) \cdot Q^2$ could not be compared directly with those observed, we take the ratio of height of the first peak to the second one as a measure of comparison. In the experimental results shown in Fig. 3 this ratio increases with the incubation time in the same manner as the ratio in the simulated curves shown in Fig. 6 increases with the number of layers of 20S disks.

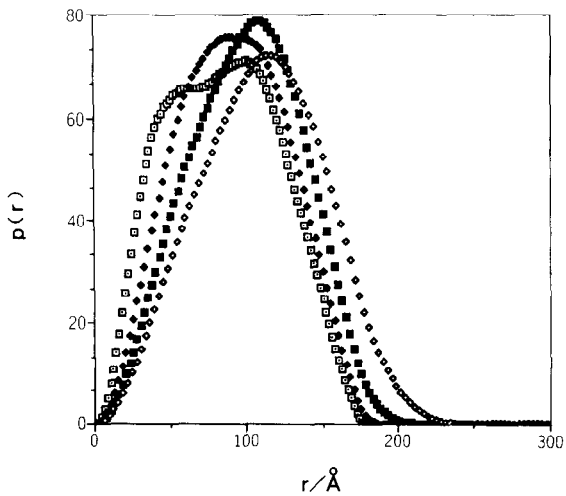

Fig. 7. Simulated distance distribution function for the model representing the multi-layered 20S disks. (⊡) 1d, (♦) 2d, (■) 3d and (◇) 4d denote a 20S disk, 2-layered 20S disk, 3-layered 20S disk and 4-layered 20S disk, respectively.

We examined the shape of curves rather than the absolute intensity in the case of the simulated $p(r)$ function, as done in the case of Kratky plot. A single-layered 20S disk exhibits a first peak at around 50 Å which is smeared by a small shoulder, adding 2-layered 20S disks in the system, and disappears according to the growth to multi-layered 20S disks. These changes in the simulated $p(r)$ function were observed in those calculated from the experimental results (compare Fig. 7 with Fig. 4).

The simulated curves of the Guinier plot, the Kratky plot and the $p(r)$ function from four types of models qualitatively reproduce the experimental curves. Here the profile changes during the simulation process from single-layered 20S disk to 4-layered 20S disk account for the elongation of the TMV assembly. As a synchronized growth of the TMV assembly cannot take place in the present reaction solutions, many degrees of aggregates are involved at any time of the measurements and the X-ray scattering is observed as an average over an ensemble. However, the time course of the R_g increase for the TMV assembly system at 20° C shown in Fig. 2, for example, is considerably similar to that obtained from the electron microscopic studies [8,9].

The present investigation proves that low-temperature quenching is a useful technique to trace biological phenomena in the order of minutes by SAXS or SANS. When the SANS measurement is combined with low-temperature quenching to observe TMV assembly, the mechanism of TMV assembly would be revealed more explicitly by the kinetics of the elongation of TMV assembly (SAXS) and that of the helical refolding of TMV-RNA (SANS).

References

[1] D.L.D. Caspar, Adv. Prot. Chem., 18 (1963) 37–121.
[2] P. Goelet, G.P. Lomonossoff, P.J.G. Butler, M.E. Akam, M.J. Gait and J. Karn, Proc. Natl. Acad. Sci. USA, 79 (1982) 5818–5822.
[3] P.J.G. Butler, J.T. Finch and D. Zimmern, Nature, 265 (1977) 217–219.
[4] G. Lebeurier, A. Nicolaieff and K.E. Richards, Proc. Natl. Acad. Sci. USA, 74 (1977) 149–153.
[5] Y. Otsuki, I. Takebe, T. Ohno, M. Fukuda and Y. Okada, Proc. Natl. Acad. Sci. USA, 74 (1977) 1913–1917.
[6] D. Zimmern and P.J.G. Butler, Cell, 11 (1977) 455–462.
[7] P.J.G. Butler and J.T. Finch, J. Mol. Biol., 78 (1973) 637–649.
[8] M. Fukuda, T. Ohno, y. Okada, Y. Otsuki and I. Takebe, Proc. Natl. Acad. Sci. USA, 75 (1978) 1727–1730.
[9] M. Fukuda and Y. Okada, Proc. Natl. Acad. Sci. USA, 84 (1987) 4035–4038.
[10] P.J.G. Butler, J. Mol. Biol., 82 (1974) 343–353.
[11] G.P. Lomonossoff and P.J.G. Butler, Eur. J. Biochem., 93 (1979) 157–164.
[12] G.P. Lomonossoff and P.J.G. Butler, FEBS Lett., 113 (1980) 271–274.
[13] H.B. Sturhmann, J. Appl. Crystallogr., 7 (1974) 173–178.
[14] Y. Hiragi, H. Inoue, Y. Sano, K. Kajiwara, T. Ueki and H. Nakatani, J. Mol. Biol., 213 (1990) 495–502.
[15] A.C.H. Durham and A. Klug, Nature New Biol., 229 (1971) 42–46.
[16] P.J.G. Butler and A. Klug, Nature New. Biol., 229 (1971) 47–50.
[17] Y. Nozu, T. Ohno and Y. Okada, J. Biochem., 68 (1970) 39–52.
[18] R. Leberman, Virology, 30 (1966) 341–341.
[19] H. Fraenkel-Conrat, B. Singer and A. Tsugita, Virology, 14 (1961)
[20] H. Fraenkel-Conrat, Virology, 4 (1957) 1–4.
[21] R. Haschemeyer, B. Singer and H. Fraenkel-Conrat, Proc. Natl. Acad. Sci. USA, 45 (1959) 313–319.
[22] Y. Nozu and Y. Okada, J. Mol. Biol., 35 (1968) 643–646.
[23] T. Ueki, Y. Hiragi, Y. Izumi, H. Tagawa, M. Kataoka, Y. Muroga, T. Matsushita and Y. Amemiya, Photon Factory Activity Report 82/83, 1983, pp. 70–71.
[24] Y. Hiragi, H. Inoue, Y. Sano, K. Kajiwara, T. Ueki, M. Kataoka, H. Tagawa, Y. Izumi, Y. Muroga and Y. Amemiya, J. Mol. Biol., 204 (1988) 129–140.
[25] A. Guinier and G. Fournet, Small-angle Scattering of X-rays, Wiley, New York, 1955.
[26] O Glatter and O. Kratky, Small Angle X-ray Scattering, Academic Press, London, 1982.
[27] I. Piltz, O. Glater and O. Kratky, Methods Enzymol., 61 (1979) 148–249.
[28] O. Glatter, Acta Phys. Austriaca, 52 (1980) 243–256.